

# Spectral function at high missing energies and momenta

T. Frick<sup>1</sup>, Kh.S.A. Hassaneen<sup>1</sup>, D. Rohe<sup>2</sup>, and H. Mütter<sup>1</sup>

<sup>1</sup> *Institut für Theoretische Physik,*

*Universität Tübingen,*

*D-72076 Tübingen, Germany and*

<sup>2</sup> *Department of Physics and Astronomy,*

*University of Basel, CH-4056 Basel, Switzerland*

The nuclear spectral function at high missing energies and momenta has been determined from a self-consistent calculation of the Green's function in nuclear matter using realistic nucleon-nucleon interactions. The results are compared with recent experimental data derived from  $(e, e'p)$  reactions on  $^{12}\text{C}$ . A rather good agreement is obtained if the Green's functions are calculated in a non-perturbative way.

## I. INTRODUCTION

The nuclear many-body problem is one of the challenging problems for quantum many-body theory. The strong components of a realistic nucleon-nucleon (NN) interaction, in particular the short-range and tensor components, induce strong correlations in the nuclear wave function. In fact, a calculation of the binding energy of nuclei, which ignores the effects of correlations beyond the Hartree-Fock or mean-field approximation, yields unbound nuclei, if realistic NN interactions are considered[1].

The investigation of such correlations should provide information about the interactions of two nucleons in the nuclear medium. Therefore considerable experimental as well as theoretical effort has been made to explore these correlations and determine their features from observables which are sensitive to correlation effects. Since one wants to investigate correlations beyond the mean field approximation, it is plausible that one tries to determine the probability for nucleons occupying states which are unoccupied in the Independent Particle Shell Model (IPSM). This implies that one tries to detect the probability of nucleons with momenta considerably above the Fermi momentum.

Attempts have been made to investigate such high-momentum components in exclusive  $(e, e'p)$  experiments, for which the energy transfer, determined from the energy of the elec-

tron and the energy of the knocked-out proton, are constrained to guarantee that the residual nucleus is in its groundstate. Using the Plane-Wave Impuls Approximation (PWIA) the momentum of the nucleon before absorbing the virtual photon can be derived from the momentum transfer from the electrons and the momentum of the outgoing proton. This means that one tries to measure the probability to remove a nucleon carrying large momentum, depositing only little energy. This probability is given by the spectral function at high momenta and small missing energies.

The experimental data on the spectral function at high momenta and small missing energies can very well be described in terms of momentum distributions derived from IPSM calculations if the theoretical strengths are quenched by a global spectroscopic factor  $Z$ [2, 3, 4]. A more detailed analysis of the spectral function showed that correlations should show up in an enhancement of the spectral function, as compared to IPSM, at high momenta *and* large missing energies[5, 6].

Due to the small cross section in this region as well as the distortion from other reaction mechanisms this requires more experimental effort[7, 8]. A calculation of the contribution from rescattering [9] of the knocked-out proton in the nucleus confirms that parallel kinematics has to be favoured compared to the perpendicular one. The correction on the spectral function measured for  $^{12}\text{C}$  at high missing momentum due to rescattering is negligible.

In this manuscript we would like to study results for the spectral function at high missing momenta and energies, which are deduced from those recent  $(e, e'p)$  experiments[7, 8], with calculations within the framework of the self-consistent Green's function approach[1, 10, 11, 12, 13]. Special attention is paid to the questions of the necessary ingredients for a calculation to provide reliable predictions for the spectral function at the energies and momenta of interest.

After this introduction we present a short review on the extraction of the spectral function in section 2. A comparison of results deduced from various approximations schemes and the experimental data is made in section 3, while the last section contains a summary and the conclusions.

## II. SPECTRAL FUNCTION

Within the framework of the self-consistent evaluation of Green's functions the spectral function in nuclear matter is calculated from the retarded nuclear self energy,

$$A(k, \omega) = \frac{-2 \text{Im } \Sigma(k, \omega + i\eta)}{[\omega - \frac{k^2}{2m} - \text{Re } \Sigma(k, \omega)]^2 + [\text{Im } \Sigma(k, \omega + i\eta)]^2}. \quad (1)$$

Different approximation schemes can be chosen for the self energy. A first method to approximate the self energy in the energy domain that can be explored in knock-out experiments is to add a perturbative two-hole-one-particle contribution to the standard Brueckner self energy,

$$\Delta \Sigma^{2h1p}(k, \omega + i\eta) = \int_{k_F}^{\infty} \frac{d^3 k'}{(2\pi)^3} \int_0^{k_F} \frac{d^3 h}{(2\pi)^3} \int_0^{k_F} \frac{d^3 h'}{(2\pi)^3} \frac{\langle \mathbf{k} \mathbf{h} | G | \mathbf{k}' \mathbf{h}' \rangle_A^2}{\omega + \epsilon_{k'} - \epsilon_h - \epsilon_{h'} + i\eta} \quad (2)$$

This expression is given by the second order diagram shown in Fig. 1 (a). Instead of the bare potential  $V$ , expression (2) contains an effective interaction, the Brueckner  $G$  matrix. The single-particle energies  $\epsilon_{k'}$  are taken from a Brueckner-Hartree-Fock spectrum.

A more sophisticated ansatz for the self energy is the ladder approximation. However, it turned out that this ladder approximation is plagued by the so-called pairing instability[16]. To circumvent the pairing instability that makes calculations impossible in the low-density system, one can use the theory of finite-temperature Green's functions. Above the transition temperature to the superfluid state, the pairing instability disappears. For low temperatures, up to  $T = 5$  MeV, the modifications that are induced by the thermal motion will be restricted to a small energy interval around the chemical potential  $\mu$ .

In the framework of self-consistent Green's functions (SCGF), the imaginary part of the ladder self energy  $\Sigma^L$  is computed from an effective two-nucleon interaction, the nuclear  $T$  matrix,

$$\begin{aligned} \text{Im} \Sigma^L(k, \omega + i\eta) &= \int \frac{d^3 k'}{(2\pi)^3} \int_{-\infty}^{+\infty} \frac{d\omega'}{2\pi} \langle \mathbf{k} \mathbf{k}' | \text{Im} T(\omega + \omega' + i\eta) | \mathbf{k} \mathbf{k}' \rangle_A \\ &\times A(k', \omega') [f(\omega') + b(\omega + \omega')]. \end{aligned} \quad (3)$$

Here,  $b(\Omega) = [e^{\beta(\Omega - 2\mu)} - 1]^{-1}$  is the Bose function and  $\beta = 1/T$  the inverse temperature. The real part of the self energy can be obtained as the sum of a Hartree-Fock contribution and an energy dependent term that is computed from the imaginary part by means of a dispersion

integral [17]. The effective interaction is determined by the following integral equation,

$$\begin{aligned} \langle q | T_{LL'}^{JST}(P, \Omega + i\eta) | q' \rangle &= \langle q | V_{LL'}^{JST} | q' \rangle + \sum_{L''} \int_0^\infty \frac{dk' k'^2}{(2\pi)^3} \langle q | V_{LL''}^{JST} | k' \rangle \\ &\times \bar{g}_{II}(P, \Omega + i\eta, k') \langle k' | T_{L''L'}^{JST}(P, \Omega + i\eta) | q' \rangle. \end{aligned} \quad (4)$$

By means of the non-interacting two-particle propagator  $g_{II}$ , the  $T$  matrix takes into account multiple off-shell scattering of particle pairs and hole pairs to all orders,

$$g_{II}(k_1, k_2, \Omega + i\eta) = \int_{-\infty}^{+\infty} \frac{d\omega}{2\pi} \int_{-\infty}^{+\infty} \frac{d\omega'}{2\pi} A(k_1, \omega) A(k_2, \omega') \frac{1 - f(\omega) - f(\omega')}{\Omega - \omega - \omega' + i\eta}. \quad (5)$$

To be used in the integral equation (4),  $g_{II}$  must be averaged over the angle between the center of mass momentum  $\mathbf{P} = \frac{1}{2}(\mathbf{k}_1 + \mathbf{k}_2)$  and the relative momentum  $\mathbf{q} = \frac{1}{2}(\mathbf{k}_1 - \mathbf{k}_2)$ .

The particles can be forced to propagate on the energy shell by introducing a quasiparticle spectrum

$$\epsilon(k) = \frac{k^2}{2m} + \text{Re}\Sigma(k, \epsilon(k)), \quad (6)$$

which yields a Dirac type spectral function,

$$A^{QP}(k, \omega) = 2\pi \delta(\omega - \epsilon(k)), \quad (7)$$

and a simple representation for  $g_{II}$  in terms of the spectrum,

$$g_{II}^{QP}(k_1, k_2, \Omega + i\eta) = \frac{1 - f(\epsilon(k_1)) - f(\epsilon(k_2))}{\Omega - \epsilon(k_1) + \epsilon(k_2) + i\eta}. \quad (8)$$

Solving for the ladder self energy  $\Sigma^{QP}$  and the  $T$  matrix in the simplified scheme by applying Eqs. (7) and (8), still, all ladders are taken into account, however, the self-consistency constraint is only fulfilled on-shell.

Since we want to discuss the influence of correlation on proton knock-out experiments, we focus our attention to the spectral function  $A(k, \omega)$  and the self-energy  $\Sigma(k, \omega)$  at energies  $\omega$  below the Fermi energy or chemical potential  $\mu$ . The time ordered diagrams presented in Fig. 1 are typical contributions to the self-energy in this energy region, representing the various approximations, which we are going to discuss. As already mentioned before, the diagram of Fig. 1 (a) represents the contribution to the self-energy of second order in the Brueckner  $G$ -matrix. The propagation of the intermediate two-hole-one-particle state is described in terms of the quasiparticle approximation to the Green's function. It represents

the contribution of Eq. (2) and we will call the approximation, which accounts for this term only, the perturbative approach.

The quasiparticle approximation goes beyond this perturbative approach in the sense that it accounts for all particle-particle hole-hole ladder diagrams, like the one displayed in Fig. 1 (b). The name quasiparticle approximation refers to the fact, that also in this approximation, the single-particle Green's functions, which enter the definition of the self-energy, are approximated by the quasiparticle approach (7).

Finally, the SCGF approximation refers to calculations, in which the self-energy (3) and the corresponding integral equation for  $T$  (4) are solved considering single-particle propagators, which account for the complete spectral function. This is represented by the double lines in the diagram of Fig. 1 (c). One may consider these double lines to represent a coupling of the propagation of particles (holes) to two-particle-one-hole (two-hole-one-particle) configurations. Therefore the diagram displayed in Fig. 1 (c) implies the admixture of  $(n+1)$ -hole- $n$ -particle configurations in the definition of the self-energy.

### III. RESULTS AND DISCUSSION

The approximations (perturbative -, quasiparticle - and SCGF approximation) just described have been employed in studies of nuclear matter at a density  $\rho$  which is one half of the empirical saturation density of nuclear matter. We have chosen this density as we want to compare the results for spectral functions with those obtained in  $(e, e'p)$  experiments on  $^{12}\text{C}$  and this density corresponds to the mean value of the particle density of this nucleus. The assumption that the spectral function of a finite nucleus can be compared to one for infinite nuclear matter is certainly not justified when considering the spectral function at low momenta and energies. In this regime the spectral function is dominated by the single-particle wave functions, which are of course quite different for infinite matter and finite nuclei. Our comparison shall focus on the spectral function at high momenta and high missing energies. The spectral function in this region is dominated by the short-range correlations, which should not be so sensitive to the global properties of the system.

Self-consistent calculations have been performed using the three approximation schemes in the sense, that for each approach we calculated the quasiparticle spectrum or the spectral functions, which enter the evaluation of the self-energy, from the corresponding self-energy.

The CD-Bonn interaction[18] has been used for the NN interaction.

As a first step it is instructive to compare the three different approximation schemes on the level of the self energy. In Fig. 2, the imaginary part of  $\Sigma$  is displayed for a small momentum that corresponds to  $k_F/5$  and a large momentum above  $2k_F$ . As explained above, the calculations are performed at different temperatures,  $T = 0$  for the perturbative approach,  $T = 2$  MeV for the SCGF solution and  $T = 5$  MeV for the quasiparticle approximation, the latter displaying a higher transition temperature to the superfluid state. Due to the finite temperature, the self energy does not go to zero at the chemical potential, which is between  $-20$  and  $-30$  MeV in the quasiparticle and the SCGF calculations.

At low momenta (left panel Fig. 2) the self-energy of the perturbative approach,  $\text{Im}\Sigma^{2h1p}$ , and the quasiparticle approximation,  $\text{Im}\Sigma^{QP}$ , exhibit a rather similar energy dependence in the tail towards negative energies, i.e. high missing energies. These two approximations also yield well pronounced maxima at around 30 MeV. The result for the SCGF approach is quite different. The maximum is reduced and the tail extends to larger missing energies. This can be understood from the fact that the SCGF approach accounts for the complete spectral function (with tails to large energies) already in calculating the self-energy, while these contributions are missing in the perturbative and the quasiparticle approximation. In other words: the SCGF approach accounts for the admixture of 3-hole-2-particle, 4-hole-3-particle etc. configurations, which are missing in the other approximations, and therefore yields an imaginary part for the self-energy and spectral strength also at higher missing energies.

This feature can also be observed in the right panel of Fig. 2, displaying the spectral function at larger momenta. In this case one furthermore observes a significant difference between the perturbative and the quasiparticle approximation: the imaginary part resulting from the perturbative calculation is much weaker than the one obtained in the calculations accounting for the particle-particle hole-hole ladders to all orders. This is a clear indication that the nonperturbative determination of the correlations is required to obtain a reliable information about the imaginary part of the self-energy or the spectral function at large momenta. Note that the scale in the right panel of Fig. 2 is reduced as compared to the left one.

The measured spectral function in the left panel of Fig. 3 provide direct evidence for the partial occupation of single particle states above the Fermi level by off-shell particles. The nuclear matter spectral function derived in the theory of SCGF is compared to the exper-

imental spectral functions for different momenta above  $k_F = 209 \text{ MeV/c}$ . The prediction derived from the calculation in nuclear matter should not be reliable at low missing energies. At these energies the spectral function should be influenced by long-range correlations, which are different in infinite matter as compared to finite nuclei. The agreement is rather good up to  $2k_F$ . For even higher momenta, the energy dependence is not well reproduced and the theoretical result tends to overshoot at high missing energies whereas for smaller energies strength is missing.

The right panel of Fig. 3 shows different theoretical calculations for a specific nucleon momentum of  $k = 410 \text{ MeV/c}$ . Compared to the data the spectral function from the CBF theory has the same tendency as the SCGF approach described above. However, the SCGF approach seems to be closer to the experimental results at high missing energies.

Further, one can compare the correlated strength from the SCGF approach to the experimental result as it was done for the CBF theory [20]. For this purpose we integrate the spectral function over momentum and energy in the correlated region above the Fermi level covered by the experiment. The lower limit of the energy in the integral has been taken as 40 MeV to avoid the contribution of the single-particle levels. The correlated strength from the SCGF theory in the integration region specified in [20] is 0.61. The experimental value is  $0.61 \pm 0.06$ , which contains a contribution from rescattering of 4 %. Good agreement is achieved.

#### IV. CONCLUSIONS

The study of the spectral function for nucleon knock-out experiments at high momenta and large missing energies seems to be an appropriate tool to explore the effect of correlations on the nuclear many-body wave function. Our study demonstrate that non-perturbative calculations are required to predict the spectral strength at high momenta. Furthermore one has to account for the admixture of configurations beyond two-hole-one-particle to obtain a reliable prediction for the energy tail of the spectral functions towards large missing energies. These ingredients are taken into account in the SCGF (self-consistent Green's functions) approach. The comparison of the spectral function derived from experimental data with the results obtained from nuclear matter calculation using SCGF indicates that the effects of short-range correlations are insensitive to the bulk structure of the nuclear system. The study

of the spectral function at low missing energies will require a more detailed investigation of long-range correlation and should be performed for the finite system.

The authors would like to thank Ingo Sick for many discussions. Also we would like to acknowledge financial support from the *Europäische Graduiertenkolleg Tübingen - Basel*, which is supported by the *Deutsche Forschungsgemeinschaft* (DFG) and the *Schweizerische Nationalfonds* (SNF).

- 
- [1] H. Mütter and A. Polls, Prog. Part. Nucl. Phys. **45**, 243 (2000).
  - [2] K.I. Blomqvist et al., Phys. Lett. **B 344**, 85 (1995).
  - [3] I. Bobeldijk et al., Phys. Rev. Lett. **73**, 2684 (1994).
  - [4] M. F. van Batenburg, Ph.D. thesis, University of Utrecht (2001).
  - [5] H. Mütter and W. H. Dickhoff, Phys. Rev. **C 49**, R17 (1994).
  - [6] H. Mütter, A. Polls and W. H. Dickhoff, Phys. Rev. **C51**,3040 (1995).
  - [7] D. Rohe, *Eur. Phys. J. A* **17**, 493 (2003) .
  - [8] D. Rohe, *Habilitationsschrift*, University of Basel (2004).
  - [9] C. Barbieri, *Proceedings 6th Workshop on e-m induced Two-Hadron Emission*, Pavia, 2003
  - [10] M. Baldo, *Nuclear Methods and the Nuclear Equation of State*, Int. Rev. of Nucl. Phys, Vol. 9 (World Scientific, Singapore, 1999).
  - [11] W. H. Dickhoff and H. Mütter, Rep. Prog. Phys. **55**, 1947 (1992).
  - [12] W.H. Dickhoff and C. Barbieri, Prog. Part. Nucl. Phys. in print, nucl-th/0402034.
  - [13] P. Božek, Phys. Rev. **C 65**, 054306 (2002).
  - [14] T. de Forest, Nucl. Phys. **A392** (1983) 232
  - [15] O. Benhar, V.J. Pandharipande and S. Pieper, private communication
  - [16] A. Ramos, A. Polls and W. H. Dickhoff, Nucl. Phys. **A 503**, 1 (1989).
  - [17] T. Frick and H. Mütter, Phys. Rev. **C 68**, 034310 (2003).
  - [18] R. Machleidt, F. Sammarruca, and Y. Song, *Phys. Rev. C* **53**, R1483 (1996)
  - [19] O. Benhar, A. Fabrocini, S. Fantoni and I. Sick, *Nucl. Phys. A* **579**, 493 (1994)
  - [20] D. Rohe et al., submitted to Phys. Rev. Lett., nucl-ex0405028.



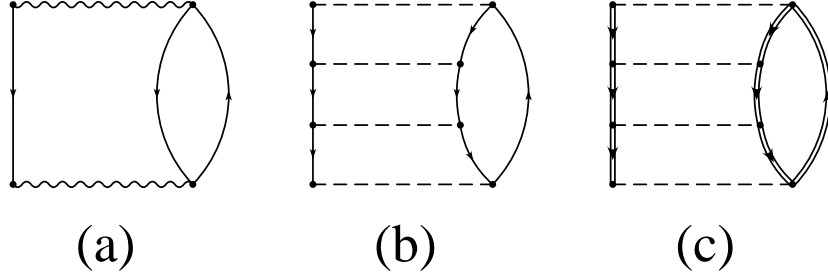


FIG. 1: Time ordered diagrams included in the different approximations for the self energy. In the second-order perturbative approximation (a), the bare potential (dashed line) is replaced by a Brueckner  $G$  matrix (wiggly line). The quasiparticle approximation includes hole-hole scattering of quasiparticles to all orders (b), and the self-consistent approximation includes hole-hole scattering also off-shell (c).

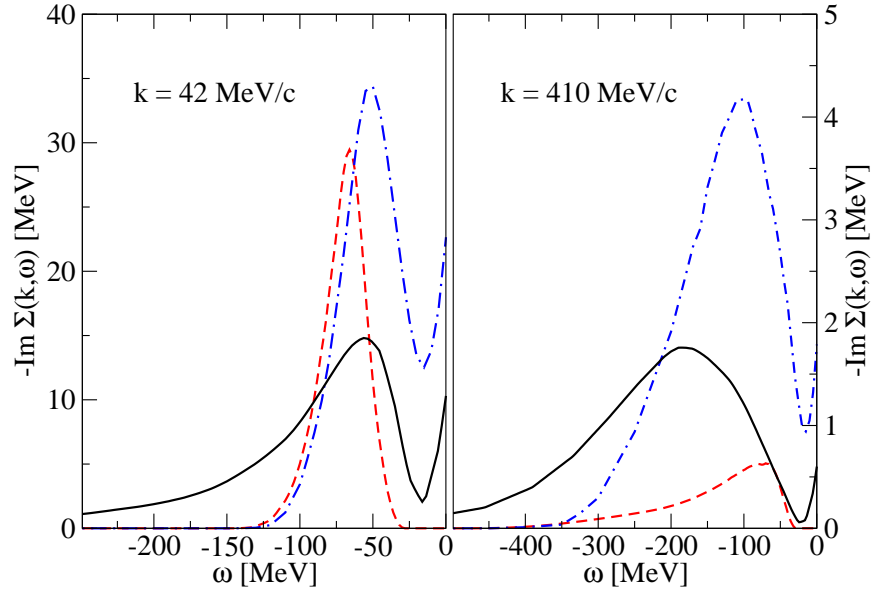


FIG. 2: (Color online) Imaginary part of the nuclear self energy in nuclear matter at  $0.5\rho_0$ . The perturbative 2h1p result (dashed line) is compared to the quasiparticle (QPGF) approximation (dash-dotted line) and the full SCGF result (solid line). The momentum is  $0.2k_F$  in the left panel and about  $2k_F$  in the right panel.

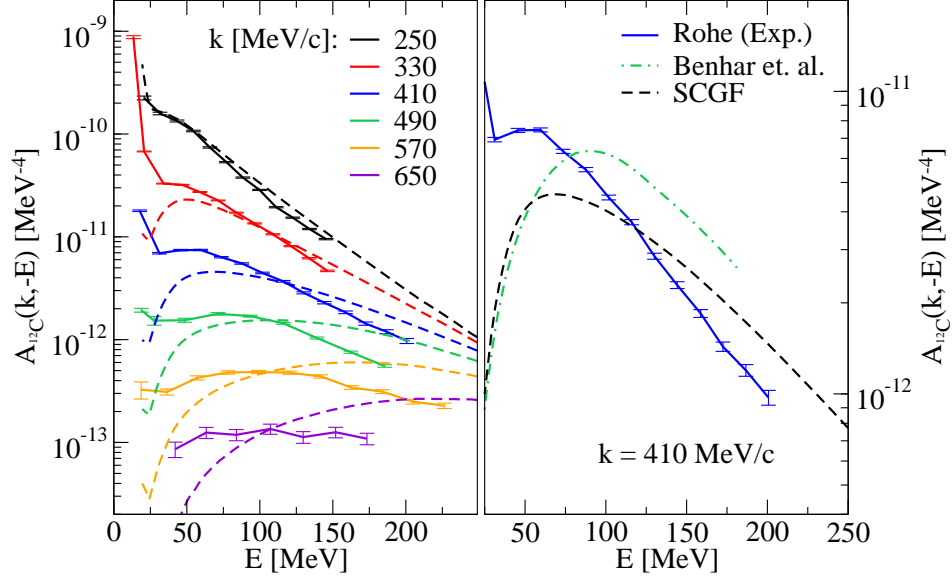


FIG. 3: (Color online) Spectral function in the  $^{12}\text{C}$  nucleus. Left panel: Experimental result for several momenta above the Fermi momentum (solid lines with error bars). The data are similar to those presented in Ref. [7], but the choice  $cc$  was used for  $\sigma_{ep}$  instead of  $cc1$ . The dashed lines represent the SCGF nuclear matter spectral function at a density of  $\rho = 0.08 \text{ fm}^{-3}$ . To compare the nuclear matter spectral function with the experimental result, it must be multiplied by a normalization factor of  $4Z(2\pi)^{-4}\rho^{-1}$ . Right panel: A comparison between the experimental result at  $k = 410 \text{ MeV}$  (solid lines with error bars), the theoretical spectral functions for a finite system by Benhar *et al.* [19] (dashed line) and the SCGF result (solid line).